First Principle Calculation of Cohesive Energy of Zirconium and Xenon Segregated Grain Boundary of UO_2

Jae Joon Kim [a], Ho Jin Ryu [a*]
[a]*Department of Nuclear and Quantum Engineering, KAIST, Daejeon 34141, Republic of Korea*
[*]*Corresponding author: hojinryu@kaist.ac.kr*

1. Introduction

Grain boundaries are the most common structural defects in UO_2 nuclear fuels and play an important role in accommodation of fission products, which serve as nucleation sites for fission gas bubbles metallic and oxide precipitates. Some of the fission products formed during normal operation are deposited at the UO_2 grain boundary. Hocking et al. gave the segregation tendency and the form of segregation of 32 different fission products in UO_2 fuel. [1] Among them are zirconium and xenon elements which exist in high concentrations in irradiated nuclear fuel and which have high tendency to segregate.

There is a lot of experimental evidence that fission products segregation weakens the grain boundaries of UO_2. [2–4] However, accurate analysis of the effect of fission products segregation on the grain boundary cohesive energy of UO_2 has not been performed yet. The grain boundary cohesive energy is particularly used in the fuel pulverization model. It is used in the calculation of threshold pressure of the intergranular bubble for grain boundary splitting. [5]

DFT is actively used to calculate material properties such as formation energy, phonon calculation, and density of state. Many groups have already conducted studies on grain boundary segregation and cohesive energy of materials using DFT calculations. [6–8] DFT analysis also has been used investigate the behavior of fission products inside nuclear fuel lattice. [9,10] Until now, however, the effect of segregation of fission products on UO_2 grain boundary cohesive energy has not been analyzed by DFT calculation.

In this study, the effect of grain boundary segregation in UO_2 of zirconium and xenon on grain boundary cohesive energy was investigated through DFT analysis. The most stable structure in which the fission products can exist at the UO_2 grain boundary was found, and energy needed to separate grain boundary was calculated in the most stable configuration. The calculated grain boundary cohesive energy can be used to derive the values such as strength, fracture toughness, and threshold pressure for grain boundary separation by intergranular bubble of high burnup nuclear fuel, and will contribute to the safety analysis of nuclear reactor.

2. Methods and Results

2.1 Computational details.

Total energy calculations by DFT were performed with the projector-argument-wave method as implemented in the Vienna *ab inito* simulation package (VASP). [11] The generalized gradient approximation (GGA) with Perdew-Burke-Ernzerhof (PBE) was used for exchange correlation functional, and the projected augmented wave (PAW) method were used to substitute core electrons of uranium, oxygen, and fission products atoms. [12–14] The Hubbard *U* correction is used to describe strongly correlated electrons in 5*f* orbital in uranium atoms. For value of U_{eff}, 3.96 eV was chosen for all conducted calculations in this study. This value is very close to the value used by Dudarev et al. [15] A plane wave basis set with a cut off energy of 500 eV and 5×5×1 *k*-point grid were used. Spin polarization was considered in all calculations. Convergence of the electronic relaxation was satisfied when the total energy change was smaller than 10^{-7} eV/atom. Structural relaxation was conducted with conjugate-gradient algorithm until the Hellmann-Feynman force are less than 0.03 eV/Å.

2.2 Grain boundary modeling and segregation site investigation for zirconium and xenon.

The unit cell for simulation including CaF_2 structure of UO_2 Σ3(111)/[110] grain boundary is presented in Figure 1. The tilt angle is 109.47°. 120 atoms were used for the simulation. Considering the symmetry, there are 3 different segregation sites in the structure and sites are marked in Figure 1.

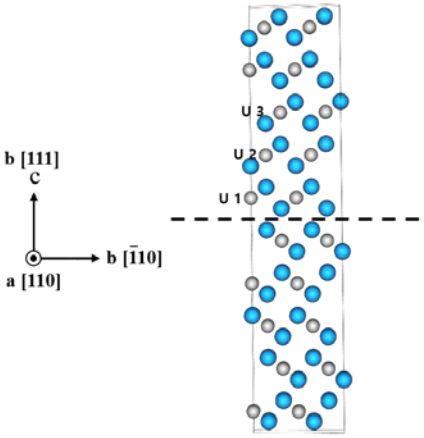

Figure 1. Σ3(111)/[110] UO_2 grain boundary.

For zirconium and xenon, the most stable segregation site was investigated by comparing the total energy of the structures segregated at each site. Figure 2 shows the total energy of the grain boundary structure in which zirconium and xenon atoms are segregated at each site.

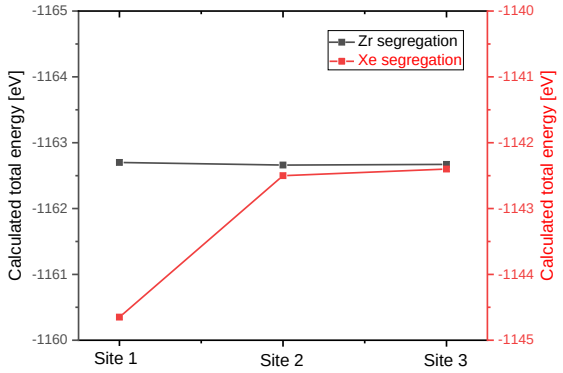

Figure 2. Comparison of total energy by segregation site.

In the case of zirconium segregation, there was little difference in total energy depending on the site, but in the case of xenon segregation, site 1 had the lowest total energy which means that site 1 is the most stable segregation site for xenon. Figure 3 shows the grain boundary structure with complete stabilization when there is no segregation atom and when zirconium and xenon are segregated at site 1. Each elements is described considering the ionic and van der Waals radius. Zirconium has tetravalent in this structure and forms ionic bonds with nearby oxygen ions. The radius of the zirconium tetravalent ion is 80 pm, and the radius of the uranium tetravalent ion is 114 pm. [16] Therefore, the oxygen ion close to the segregated zirconium atom moves toward the zirconium. Because of the relatively small ionic radius of zirconium and the characteristic of Σ3(111)/[110] with high structural similarity to the monocrystal, the difference in total energy according to the segregation site is small. In the case of xenon, it does not form chemical bond with surrounding elements according to the characteristics of the inert gas. The van der Waals radius of xenon is 216 pm, which is even larger than the radius of uranium tetravalent ion. [17] Therefore, contrary to zirconium, it can be seen that the adjacent oxygen ions move slightly away from the segregated xenon atom. Considering this spatial distortion, segregation near the grain boundary where atoms are least dense is the most energetically stable for xenon. Therefore xenon has the lowest total energy when it exists at site 1 compared to when it exists at other sites.

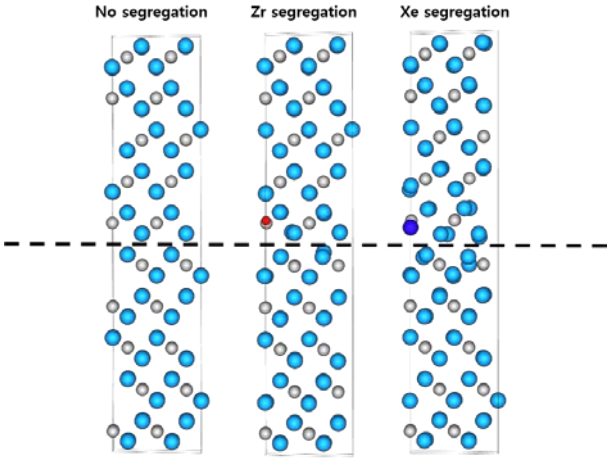

Figure 3. Segregated grain boundary structure after full relaxation.

REFERENCES

[1] W.H. Hocking, A.M. Duclos, L.H. Johnson, Study of fission-product segregation in used CANDU fuel by X-ray photoelectron spectroscopy (XPS) II, J. Nucl. Mater. 209 (1994) 1–26. https://doi.org/10.1016/0022-3115(94)90243-7.

[2] R. Henry, I. Zacharie-Aubrun, T. Blay, N. Tarisien, S. Chalal, X. Iltis, J.M. Gatt, C. Langlois, S. Meille, Irradiation effects on the fracture properties of UO2 fuels studied by micro-mechanical testing, J. Nucl. Mater. (2020). https://doi.org/10.1016/j.jnucmat.2020.152179.

[3] R. Henry, I. Zacharie-Aubrun, T. Blay, S. Chalal, J.M. Gatt, C. Langlois, S. Meille, Fracture properties of an irradiated PWR UO2 fuel evaluated by micro-cantilever bending tests, J. Nucl. Mater. (2020). https://doi.org/10.1016/j.jnucmat.2020.152209.

[4] J.A. Turnbull, S.K. Yagnik, M. Hirai, D.M. Staicu, C.T. Walkert, An assessment of the fuel pulverization threshold during LOCA-type temperature transients, Nucl. Sci. Eng. (2015). https://doi.org/10.13182/NSE14-20.

[5] L.O. Jernkvist, A review of analytical criteria for fission gas induced fragmentation of oxide fuel in accident conditions, Prog. Nucl. Energy. (2020). https://doi.org/10.1016/j.pnucene.2019.103188.

[6] Y.J. Hu, Y. Wang, W.Y. Wang, K.A. Darling, L.J. Kecskes, Z.K. Liu, Solute effects on the Σ3 111[11-0] tilt grain boundary in BCC Fe: Grain boundary segregation, stability, and embrittlement, Comput. Mater. Sci. (2020). https://doi.org/10.1016/j.commatsci.2019.109271.

[7] J. Li, C. Zhang, L. Xu, Z. Zhang, N. Dong, Y. Liu, J. Wang, Y. Zhang, L. Ling, P. Han, Effects of B on the segregation of Mo at the Fe-Cr-NiΣ5(210) grain boundary, Phys. B Condens. Matter. (2019). https://doi.org/10.1016/j.physb.2019.05.018.

[8] M. Yamaguchi, First-principles study on the grain boundary embrittlement of metals by solute

segregation: Part I. iron (Fe)-solute (B, C, P, and S) systems, in: Metall. Mater. Trans. A Phys. Metall. Mater. Sci., 2011. https://doi.org/10.1007/s11661-010-0381-5.

[9] D.A. Andersson, B.P. Uberuaga, P. V. Nerikar, C. Unal, C.R. Stanek, U and Xe transport in UO2±x: Density functional theory calculations, Phys. Rev. B - Condens. Matter Mater. Phys. (2011). https://doi.org/10.1103/PhysRevB.84.054105.

[10] G. Brillant, F. Gupta, A. Pasturel, Investigation of molybdenum and caesium behaviour in urania by ab initio calculations, J. Phys. Condens. Matter. (2009). https://doi.org/10.1088/0953-8984/21/28/285602.

[11] G. Kresse, J. Furthmiiller, Efficiency of ab-initio total energy calculations for metals and semiconductors, Comput. Mater. Sci. (1996).

[12] J.P. Perdew, K. Burke, M. Ernzerhof, Generalized gradient approximation made simple, Phys. Rev. Lett. (1996). https://doi.org/10.1103/PhysRevLett.77.3865.

[13] J.P. Perdew, K. Burke, Comparison shopping for a gradient-corrected density functional, Int. J. Quantum Chem. (1996). https://doi.org/10.1002/(SICI)1097-461X(1996)57:3<309::AID-QUA4>3.0.CO;2-1.

[14] P.E. Blöchl, Projector augmented-wave method, Phys. Rev. B. (1994). https://doi.org/10.1103/PhysRevB.50.17953.

[15] M.R. Castell, S.L. Dudarev, C. Muggelberg, A.P. Sutton, G.A.D. Briggs, D.T. Goddard, Surface structure and bonding in the strongly correlated metal oxides NiO and UO2, J. Vac. Sci. Technol. A Vacuum, Surfaces, Film. (1998). https://doi.org/10.1116/1.581232.

[16] R.D. Shannon, Revised effective ionic radii and systematic studies of interatomic distances in halides and chalcogenides, Acta Crystallogr. Sect. A. (1976). https://doi.org/10.1107/S0567739476001551.

[17] S.S. Batsanov, Van der Waals radii of elements, Inorg. Mater. (2001). https://doi.org/10.1023/A:1011625728803.